PHYSICAL REVIEW C VOLUME 3, NUMBER 6 JUNE 1971

Effective Operators and the Analysis of Single-Nucleon Transfer Reactions on Closed-Shell Nuclei*

D. R. Bes and R. A. Broglia†
University of Minnesota, School of Physics, Minneapolis, Minnesota 55455
and Los Alamos Scientific Laboratory, University of California, Los Alamos, New Mexico 87544
(Received 12 October 1970)

Spectroscopic factors for the one-body stripping and pickup reactions on ^{208}Pb are analyzed within the particle-vibration-coupling model that was developed in the first paper of this series. The calculation of the transfer amplitudes is performed up to third-order perturbation theory. A comparison with recent experimental data is carried out.

I. INTRODUCTION

In the last few years it has become more apparent that realizations of concepts such as closed-shell or single-particle states are nowhere found in the Periodic Table, in the sense of the extreme single-particle description.[1] This has been the outcome of improvements in the experimental techniques resulting from the new accelerators. Both one-particle stripping and pickup reactions have been most useful in learning about the distribution of single-particle strength as well as about ground-state correlations or, as usually called in these kinds of experiments, "core excitations." Good examples of the above statements are provided by the systematic experimental information[2] obtained on the $f_{7/2}$ nuclei; in particular, on the Ca isotopes. The interpretation of the data is usually simpler for double-closed-shell targets (such as ^{40}Ca or ^{48}Ca).

Definite theoretical problems have to be solved before the experimental cross sections can be interpreted as single-particle strengths. The three most important problems are:

(1) The extraction of spectroscopic factors from the measured cross sections. This is customarily done in the distorted-wave Born approximation (DWBA), using the separation-energy prescription to calculate the radial form factor. Although the DWBA seems to be a rather successful way of extracting spectroscopic information from nuclear reactions, the separation-energy prescription has little justification and may introduce considerable uncertainty in the spectroscopic factor associated with weak transitions.

(2) The extraction, through the spectroscopic factors, of quantitative information on both the single-particle states and their admixtures with more complicated states (usually called nonpickup or nonstripping components). For this one needs a good description of the final excited states in the odd nucleus, which depend on the description of the low-lying collective states of the closed-shell system. These states are not necessarily in the system N_0. If pairing modes are considered, they would include states of the $N_0 \pm 2$ nuclei. It is easy to see that this problem implies a requirement of self-consistency. At the same time, the modification of the single-particle states due to their coupling to the collective states of N_0 nucleons implies that effective transfer operators should be used. These operators are related to the reaction cross sections as the effective energy matrix elements are to the energy.

(3) If two-step processes are included,[3] the two problems listed above are intimately related and cannot be treated separately.

Some of these problems have been considered by Hamamoto,[4] based on the perturbation treatment of particle vibration suggested by Mottelson.[5]

In this paper we present, following Refs. 4 and 5, a systematic way of dealing with problem 2, concerning both the final-state wave functions and the use of effective transfer operators. Problem 1 will be discussed elsewhere[6] using the approach presented in the work of Ibarra and Bayman.[7] The basis of the model to be used was discussed in an earlier paper.[8] Though the methods described below apply to any closed-shell system, we concentrate our attention on the case of single-neutron stripping and pickup on ^{208}Pb.

In Sec. II, the description of the $N_0 \pm 1$ states

given in Ref. 8 is briefly summarized. In Sec. III, the matrix elements of the effective one-nucleon-transfer operator are derived. Section IV contains the results of the calculation and a comparison with available experimental data.

Other approaches have also been used in order to couple particles and closed-shell vibrations.[9] However, the comparison between the corresponding results and our predictions is not easy to perform, because the main emphasis in most of these studies has been on the modifications of the properties of single-particle states.

II. DISCUSSION OF THE MODEL

The low-lying states of the $N_0 \pm 1$ system correspond to single-particle (hole) states $|j\rangle$. We use the notation $|k\rangle$ ($|i\rangle$) for states above (below) the Fermi surface. In the $N_0 + 1$ nucleus, the next states are two-particle–one-hole (2p-1h) states. To describe them we use a set of states

$$|n2\lambda; i; JM\rangle = [\beta_n^\dagger(2\lambda) b_i]^J_M |0\rangle , \tag{1a}$$

$$|n0\lambda; k; JM\rangle = [\beta_n^\dagger(0\lambda) b_k^\dagger]^J_M |0\rangle . \tag{1b}$$

In the $N_0 - 1$ system, we similarly represent the (2h-1p) states by

$$|n -2\lambda; k; JM\rangle = [\beta_n^\dagger(-2\lambda) b_k^\dagger]^J_M |0\rangle , \tag{2a}$$

$$|n0\lambda; i; JM\rangle = [\beta_n^\dagger(0\lambda) b_i]^J_M |0\rangle . \tag{2b}$$

The operator $b_j^\dagger$ creates a particle in a state with angular momentum j. The collective phonons considered are of the particle-hole type and of the multipole-pairing type. The corresponding creation operators, $\beta_n^\dagger(0\lambda)$ and $\beta_n^\dagger(\pm 2\lambda)$, are defined in Appendix A. The label α is the transfer quantum number, while λ represents the phonon angular momentum. These operators define, together with the particle operators b_j, the ground state

$$\beta_n(\alpha\lambda)|0\rangle = b_j|0\rangle = 0 . \tag{3}$$

The Hamiltonians that couple the odd particle to the vibrating core are

$$h(0\lambda) = -\frac{X_\lambda}{2} \sum_\mu [(Q_{\lambda\mu})_{\rm coll} Q_{\lambda\mu}^\dagger + Q_{\lambda\mu}(Q_{\lambda\mu}^\dagger)_{\rm coll}] \tag{4}$$

and

$$h(2\lambda) = -G_\lambda 2\pi(2\lambda + 1) \times \sum_\mu [(P_{\lambda\mu}^\dagger)_{\rm coll} P_{\lambda\mu} + P_{\lambda\mu}^\dagger (P_{\lambda\mu})_{\rm coll}] . \tag{5}$$

Equation (4) represents the coupling Hamiltonian between a particle and a surface vibration, and Eq. (5) represents the coupling between a particle and a pairing vibration. The collective operators are equal to

$$(Q_{\lambda\mu})_{\rm coll} = -\frac{(2\lambda+1)^{1/2}}{X_\lambda} \times \sum_n \Lambda_n(0\lambda)[\beta_n^\dagger(0\lambda\mu) + (-1)^{\lambda-\mu}\beta_n^\dagger(0\lambda-\mu)] , \tag{6}$$

$$(P_{\lambda\mu})_{\rm coll} = -\frac{1}{4\pi G_\lambda (2\lambda+1)^{1/2}} \sum_n [\Lambda_n(2\lambda)\beta_n^\dagger(2\lambda\mu) + (-1)^{\lambda-\mu}\Lambda(-2\lambda)\beta_n(-2\lambda-\mu)] . \tag{7}$$

They describe the collective variable in the usual macroscopic description. The quantity $\Lambda_n(\alpha\lambda)$ is the coupling strength. On the other hand, $Q_{\lambda\mu}^\dagger$ and $P_{\lambda\mu}^\dagger$ represent the particle degrees of freedom and are equal to

$$Q_{\lambda\mu}^\dagger = -\frac{2}{(2\lambda+1)^{1/2}} \times \sum_{k,i} M(ki;\lambda)[\beta^\dagger(ki;0\lambda\mu) + (-1)^{\lambda-\mu}\beta(ki;0\lambda-\mu)] , \tag{8}$$

$$P_{\lambda\mu}^\dagger = -\frac{2}{(2\lambda+1)^{1/2}} \left[\sum_{k_1 \geq k_2} \frac{M(k_1k_2;\lambda)}{(1+\delta_{12})^{1/2}} \beta^\dagger(k_1k_2;2\lambda\mu) + \sum_{i_1 \geq i_2} \frac{M(i_1i_2;\lambda)}{(1+\delta_{12})^{1/2}} (-1)^{\lambda-\mu}\beta(i_1i_2;-2\lambda-\mu) \right] . \tag{9}$$

The operators $\beta^\dagger(j_1j_2;\alpha\lambda\mu)$ create a single particle-hole pair ($\alpha = 0$) or a single two-particle ($\alpha = 2$) or two-hole ($\alpha = -2$) pair. The quantities $M(j_1j_2;\lambda)$ are defined as

$$M(j_1j_2;\lambda) = i^{l_{j_2} - l_{j_1} + \lambda} \langle j_1 \| f_\lambda(r) Y_\lambda \| j_2 \rangle = (-1)^{j_1 - j_2 + \lambda} M(j_2j_1;\lambda) . \tag{10}$$

The actual calculations are carried with $f_\lambda(r) = r^\lambda$. [See Eq. (39) of Ref. 8.] The basic matrix elements [linear in $\Lambda_n(\alpha\lambda)$] of the Hamiltonians [Eqs. (4) and (5)] are given in Appendix A. In what follows we make use of them to calculate the single-particle stripping and pickup spectroscopic factors to the 2p-1h (1p-2h) states of the nuclei ^{207,209}Pb below 4 MeV of excitation. This is done up to third order in the Λ's. For a more detailed discussion of the model discussed above, we refer to Ref. 8. Explicit expressions are only given for the stripping processes. The modifications for the pickup reaction can be easily obtained.

III. CALCULATION OF THE EFFECTIVE OPERATOR

A. First-Order Processes

The first-order processes leading to 2p-1h states are represented in Fig. 1. If the stripping

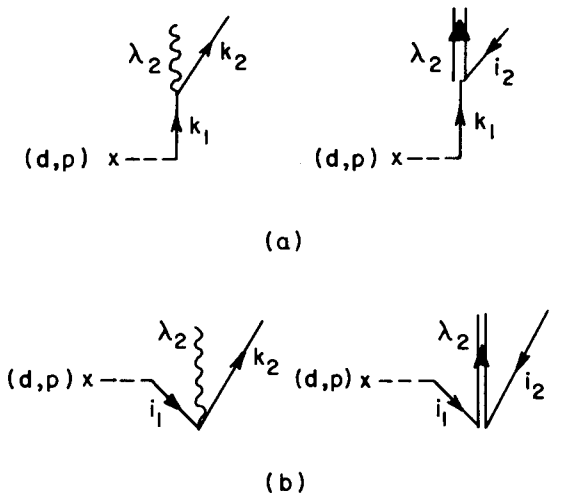

FIG. 1. First-order graphs representing the one-body stripping reactions on closed-shell nuclei. Graphs (a) correspond to the stripping to states having the same spin and parity as the single-particle states above the Fermi level. Graphs (b) represent transitions to states having the same spin and parity as the single-parity states below the Fermi surface.

reaction introduces a particle in the shell above, the particle occupies an empty single-particle state which subsequently decays into a 2p-1h state through a first-order process [Fig. 1(a)]. The corresponding spectroscopic amplitudes are given by

$$\langle n0\lambda; k_2; km|b_{km}{}^{\dagger}|0\rangle = -\Lambda_n(0\lambda)\left(\frac{2\lambda+1}{2k+1}\right)^{1/2}\frac{M(k_2k;\lambda)}{\epsilon_k+\epsilon_{p_{1/2}}-\epsilon_{g_{9/2}}-\epsilon_{k_2}+\Delta W_n(0\lambda)}, \tag{11}$$

$$\langle n2\lambda; i_2; km|b_{km}{}^{\dagger}|0\rangle = \Lambda_n(2\lambda)\left(\frac{2\lambda+1}{2k+1}\right)^{1/2}\frac{M(i_2k;\lambda)}{\epsilon_k+\epsilon_{i_2}-2\epsilon_{g_{9/2}}+\Delta W_n(2\lambda)}.$$

The energy differences $\Delta W_n(\alpha\lambda)$ measure the change in energy of two-particle, two-hole, or particle-hole states induced by the residual interaction in the corresponding $(\alpha\lambda)$ channel considered [see Eq. (30) of Ref. 8].

If, however, the particle is stripped into an occupied state, it is necessary to perturb first the vacuum state, since only then it is possible to fill the corresponding hole [Fig. 1(b)]. In this case, the amplitudes are given by

$$\langle n0\lambda; k_2; im|b_{im}{}^{\dagger}|0\rangle = \Lambda_n(0\lambda)\left(\frac{2\lambda+1}{2i+1}\right)^{1/2}\frac{M(k_2i;\lambda)}{\epsilon_{k_2}+\epsilon_{g_{9/2}}-\epsilon_{p_{1/2}}-\epsilon_i-\Delta W_n(0\lambda)}, \tag{12}$$

$$\langle n2\lambda; i_2; im|b_{im}{}^{\dagger}|0\rangle = -\Lambda_n(2\lambda)\left(\frac{2\lambda+1}{2i+1}\right)^{1/2}\frac{M(i_2i;\lambda)}{2\epsilon_{g_{9/2}}-\epsilon_{i_2}-\epsilon_{p_{1/2}}-\Delta W_n(2\lambda)}.$$

The matrix elements [Eq. (12)] give a measure of how ground-state correlations of the closed-shell system are affected by the presence of the odd particle. In other words, they measure the *rigidity* of the closed-shell system. In particular, the single-stripping process to 2p-1h states having the same spin and parity as the 1h states *are not an absolute measure* of the ground-state correlations in the closed shell, since additional types of correlations may exist and yet be undetected in this specific reaction, provided that the presence of the odd particle does not affect such correlations.

It has been systematically shown[10] that in the lowest nonvanishing order, the Hamiltonians [Eqs. (4) and (5)] yield the same results as the random-phase approximation (RPA). The one-body transfer to 2p-1h states is no exception to this statement. In the RPA we write the correlated vacuum $|0\rangle$ as a product of operators acting on the closed-shell state $|0\rangle_{cs}$,

$$|0\rangle = \prod_{n\alpha\lambda} G_n(\alpha\lambda)|0\rangle_{cs},$$

$$G_n(2\lambda) = a_{n2\lambda}\exp\left\{\sum_{\substack{k_1\geq k_2\\ i_1\geq i_2}}\eta(k_1k_2;i_1i_2;n2\lambda)[\beta^{\dagger}(k_1k_2;2\lambda)\beta^{\dagger}(i_1i_2;-2\lambda)]_0^0\right\}, \tag{13}$$

$$G_n(0\lambda) = a_{n0\lambda}\exp\left\{\sum_{(k_1i_1)\geq(k_2i_2)}\eta(k_1i_1,k_2i_2;n0\lambda)[\beta^{\dagger}(k_1i_1;0\lambda)\beta^{\dagger}(k_2i_2;0\lambda)]_0^0\right\}.$$

Here $a_{n\alpha\lambda}$ are normalization constants. The coefficients $\eta(j_1j_2,j_3j_4;n\alpha\lambda)$ are determined by the conditions

$$\beta_n(\alpha\lambda\mu)G_n(\alpha\lambda)|0\rangle_{cs} = 0, \tag{14}$$

which yield the linear equations

$$\sum_{k_1 \geq k_2} \eta(k_1 k_2; i_1 i_2; n2\lambda) d_n(k_1 k_2, 2\lambda) = (2\lambda+1)^{1/2} d_n(i_1 i_2, 2\lambda),$$

$$\sum_{k_1 i_1} (1+\delta_{k_1 k_2}\delta_{i_1 i_2})\eta(k_1 i_1, k_2 i_2; n0\lambda) d_n(k_1 i_1; 0\lambda) = (2\lambda+1)^{1/2} d_n(i_2 k_2, 0\lambda). \tag{15}$$

Using Eq. (13) and some algebra we may show

$$b_{im}{}^{\dagger} G_n(2\lambda)|0\rangle_{cs} = \frac{1}{(2i+1)^{1/2}} \sum_{i_2} (1+\delta_{i_1 i_2})^{1/2} \sum_{k_1 \geq k_2} \eta(k_1 k_2, i_1 i_2; n2\lambda) [\beta^{\dagger}(k_1 k_2, 2\lambda) b_{i_2}]^i_m G_n(2\lambda)|0\rangle_{cs}$$

$$= \frac{1}{(2i+1)^{1/2}} \sum_{n_1 i_2} (1+\delta_{i_1 i_2})^{1/2} \Big\{ \sum_{k_1 \geq k_2} \eta(k_1 k_2, i_1 i_2; n2\lambda) d_n(k_1 k_2, 2\lambda) \Big\} [\beta_n{}^{\dagger}(2\lambda) b_{i_2}]^i_m G_n(2\lambda)|0\rangle_{cs}, \tag{16}$$

which together with Eq. (15) gives

$$b_{im}{}^{\dagger} G_n(2\lambda)|0\rangle = \left(\frac{2\lambda+1}{2i+1}\right)^{1/2} \sum_{n_1 i_2} (1+\delta_{i_1 i_2})^{1/2} d_n(i i_2, 2\lambda) [\beta_n{}^{\dagger}(2\lambda) b_{i_2}]^i_m G_n(2\lambda)|0\rangle_{cs}.$$

Similarly we obtain

$$b_{im}{}^{\dagger} G_n(0\lambda)|0\rangle_{cs} = \left(\frac{2\lambda+1}{2i+1}\right)^{1/2} \sum_{n,k} d_n(ik, 0\lambda) [\beta_n{}^{\dagger}(0\lambda) b_k{}^{\dagger}]^i_m G_n(0\lambda)|0\rangle_{cs},$$

and therefore,

$$b_{im}{}^{\dagger}|0\rangle = \sum_{n\alpha\lambda} \Big[\prod_{(n'\alpha'\lambda') \neq (n\alpha\lambda)} G_{n'}(\alpha'\lambda') \Big] b_{im}{}^{\dagger} G_n(\alpha\lambda)|0\rangle_{cs}$$

$$= \sum_{n\alpha\lambda} \left(\frac{2\lambda+1}{2i+1}\right)^{1/2} \sum_j d_n(ij, \alpha\lambda)(1+\delta_{i,j})^{1/2} |n\alpha\lambda, j, im\rangle. \tag{17}$$

Using the expressions given in Eq. (5) of Ref. 8 for the coefficients $d_n(j_1 j_2, \alpha\lambda)$, we immediately obtain Eq. (12).

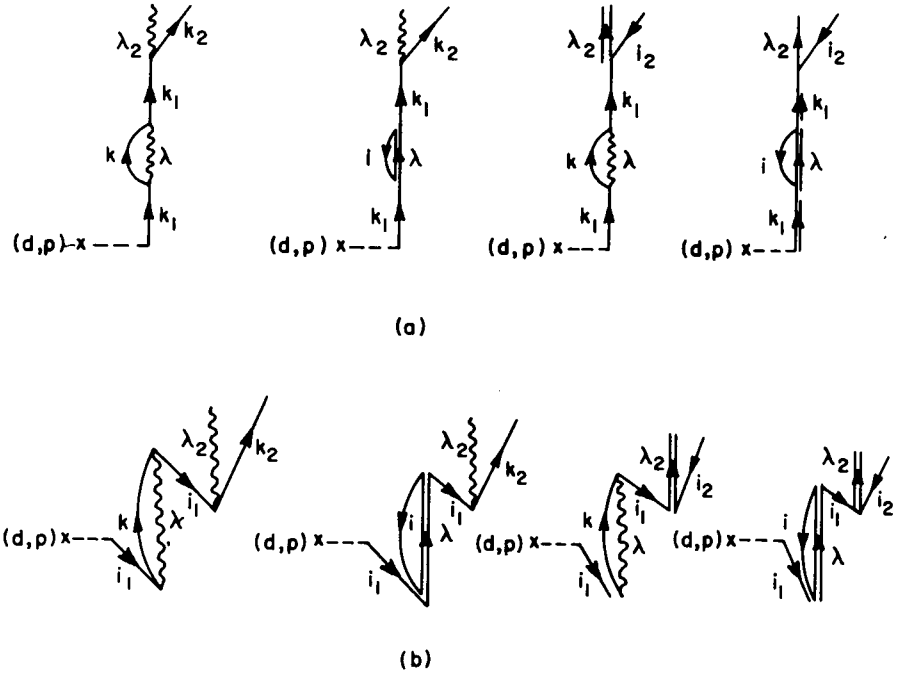

FIG. 2. Third-order graphs representing the one-body stripping reactions on closed-shell nuclei. These graphs take into account self-energy processes in the transferred particle. The distinction between graphs of type (a) and (b) Is the same as in Fig. 1.

B. Third-Order Processes

Since the 2p-1h states are mixed by the coupling Hamiltonians [Eqs. (4) and (5)] through second-order processes, we trivially obtain some third-order contributions by adding to the upper end of the graphs in Fig. 1 those graphs corresponding to the interaction between 2p-1h states (Fig. 6 of Ref. 8). The resultant graphs are given in Figs. 2 and 3. Each of these graphs gives rise to a possible maximum of $\frac{1}{2}(4!)=12$ graphs, corresponding to the permutation of the order in which the three interactions and the introduction of the particle takes place [the factor $\frac{1}{2}$ appears because graphs (b) are already obtainable from graphs (a) by a permutation in the time ordering].

Some graphs which may be derived from those explicitly given are identically zero in the present case. This is due to the fact that, in our case, single-particle states $b_k^\dagger|0\rangle$ have different spin and/or parities than the single-hole states $b_i^\dagger|0\rangle$. For instance, the graph that can be obtained from the first of the graphs 2(b) by changing the order of the last two interactions, vanishes. Finally, it is easy to check that each graph in Fig. 2 gives rise to another five contributions which, in principle, do not vanish. In the analytic expression of the effective one-particle-transfer operator corresponding to each of these contributions, we have the same numerators with a phase depending on the number of hole lines. We only give here the explicit contribution of those graphs represented in Fig. 2. Both the energy denominators and the phase can be easily obtained in other cases according to the rules of perturbation theory. For graphs[11] [2(a)],

$$\langle n_2 0\lambda_2; k_2; k_1 m|B_{k_1 m}{}^\dagger|0\rangle = -\Lambda_{n_2}(0\lambda)\left(\frac{2\lambda_2+1}{2k_1+1}\right)^{1/2}\frac{M(k_2k_1;\lambda_2)}{[\epsilon_{k_1}-\epsilon_{k_2}-\epsilon_{g_{9/2}}+\epsilon_{p_{1/2}}+\Delta W_n(0\lambda)]^2}$$
$$\times\left[\sum_{n,\lambda,i}\frac{(2\lambda+1)\Lambda_n{}^2(0\lambda)M^2(k_1k;\lambda)}{\epsilon_k-\epsilon_{k_2}+\Delta W_{n_2}(0\lambda)-\Delta W_n(0\lambda)}+\sum_{n,\lambda,i}\frac{(2\lambda+1)\Lambda_n{}^2(2\lambda)M^2(k_1i;\lambda)}{\epsilon_{g_{9/2}}-\epsilon_{k_2}+\epsilon_{p_{1/2}}-\epsilon_i+\Delta W_{n_2}(0\lambda_2)-\Delta W_n(2\lambda)}\right], \tag{18}$$

$$\langle n_2 2\lambda_2; i_2; k_1 m|B_{k_1 m}{}^\dagger|0\rangle = \Lambda(2\lambda_2)\left(\frac{2\lambda_2+1}{2k_1+1}\right)^{1/2}\frac{M(i_2k_1;\lambda_2)}{[\epsilon_{k_1}+\epsilon_{i_2}-2\epsilon_{g_{9/2}}+\Delta W_{n_2}(2\lambda_2)]^2}$$
$$\times\left[\sum_{n,\lambda,i}\frac{(2\lambda+1)\Lambda_n{}^2(2\lambda)M^2(k_1i;\lambda)}{\epsilon_{i_2}-\epsilon_i+\Delta W_{n_2}(2\lambda_2)-\Delta W_n(0\lambda)}+\sum_{n,\lambda,k}\frac{(2\lambda+1)\Lambda_n{}^2(0\lambda)M^2(k_1k;\lambda)}{\epsilon_k-\epsilon_{g_{9/2}}+\epsilon_{i_2}-\epsilon_{p_{1/2}}+\Delta W_{n_2}(2\lambda_2)-\Delta W_n(0\lambda)}\right]. \tag{19}$$

In the case of graphs 2(b), the matrix elements of the effective operator are

$$\langle n_2 0\lambda_2; k_2; i_1 m|B_{i_1 m}{}^\dagger|0\rangle = -\Lambda(0\lambda_2)\left(\frac{2\lambda_2+1}{2i_1+1}\right)^{1/2}M(k_2i;\lambda_2)$$
$$\times\left\{\sum_{n,\lambda,k}\frac{(2\lambda+1)\Lambda_n{}^2(0\lambda)M^2(i_1k;\lambda)}{[\epsilon_k+\epsilon_{g_{9/2}}-\epsilon_{i_1}-\epsilon_{p_{1/2}}-\Delta W_n(0\lambda)]^2[\epsilon_k-\epsilon_{k_2}+\Delta W_{n_2}(0\lambda)-\Delta W_n(0\lambda)]}\right.$$
$$\left.+\sum_{n,\lambda,k}\frac{(2\lambda+1)\Lambda_n{}^2(2\lambda)M^2(i_1i;\lambda)}{[2\epsilon_{g_{9/2}}-\epsilon_i-\epsilon_{i_1}-\Delta W_n(2\lambda)]^2[\epsilon_{g_{9/2}}-\epsilon_{k_2}+\epsilon_{p_{1/2}}-\epsilon_i+\Delta W_{n_2}(0\lambda_2)-\Delta W_n(2\lambda)]}\right\}, \tag{20}$$

$$\langle n_2 2\lambda_2, i_2; i_1 m|B_{i_1 m}{}^\dagger|0\rangle = \Lambda_n(2\lambda_2)\left(\frac{2\lambda_2+1}{2i_1+1}\right)^{1/2}M(i_2i;\lambda_2)$$
$$\times\left\{\sum_{n,\lambda,i}\frac{(2\lambda+1)\Lambda_n{}^2(2\lambda)M^2(i_1i;\lambda)}{[2\epsilon_{g_{9/2}}-\epsilon_{i_1}-\epsilon_i-\Delta W_n(2\lambda)]^2[\epsilon_{i_2}-\epsilon_i+\Delta W_{n_2}(2\lambda_2)-\Delta W_n(2\lambda)]}\right.$$
$$\left.+\sum_{n,\lambda,k}\frac{(2\lambda+1)\Lambda_n{}^2(0\lambda)M^2(i_1k;\lambda)}{[\epsilon_k+\epsilon_{g_{9/2}}-\epsilon_{i_1}-\epsilon_{p_{1/2}}-\Delta W_n(0\lambda)]^2[\epsilon_k-\epsilon_{p_{1/2}}+\epsilon_{i_2}-\epsilon_{g_{9/2}}-\Delta W_n(0\lambda)+\Delta W_{n_2}(2\lambda_2)]}\right\}. \tag{21}$$

The existence of the graphs in Fig. 3, or the existence of graphs (a), (b), (f), and (g) in Fig. 6 of Ref. 8, is required to take care of the fact that our basic set of states is overcomplete. Since the subset of states with $\alpha=2$ is not overcomplete, there is only one contribution in Fig. 3 if the final state has a pairing phonon. Each of the graphs in Fig. 3 gives rise to 12 different ones (including itself). The matrix elements corresponding to Fig. 3 are

$$\langle n_2 0\lambda_2, k_2; k_1 m|B_{k_1 m}{}^{\dagger}|0\rangle = \Lambda_{n_2}(0\lambda_2)\left(\frac{2\lambda_2+1}{2k_1+1}\right)^{1/2}\frac{1}{\epsilon_{k_1}-\epsilon_{k_2}-\epsilon_{g_{9/2}}+\epsilon_{p_{1/2}}+\Delta W_{n_2}(0\lambda_2)}$$

$$\times\left(\sum_{n,\lambda,k,k'}\frac{(2\lambda+1)\Lambda_n{}^2(0\lambda)\begin{Bmatrix}k & k_2 & \lambda\\ k_1 & k' & \lambda_2\end{Bmatrix}M(k_2k;\lambda)M(k'k;\lambda_2)M(k'k_1;\lambda)}{[\epsilon_{k'}-\epsilon_{k_2}+\Delta W_{n_2}(0\lambda_2)-\Delta W_n(0\lambda)][\epsilon_k+\epsilon_{g_{9/2}}-\epsilon_{k_2}-\epsilon_{p_{1/2}}-\Delta W_n(0\lambda)]}\right.$$

$$\left.+\sum_{n,\lambda,i,i'}\frac{(2\lambda+1)\Lambda_n{}^2(2\lambda)\begin{Bmatrix}i & k_2 & \lambda\\ k_1 & i' & \lambda_2\end{Bmatrix}M(k_2i;\lambda)M(i'i;\lambda_2)M(i'k_1;\lambda)}{[\epsilon_{g_{9/2}}-\epsilon_{k_2}+\epsilon_{p_{1/2}}-\epsilon_{i'}+\Delta W_{n_2}(0\lambda_2)-\Delta W_n(2\lambda)][2\epsilon_{g_{9/2}}-\epsilon_{k_2}-\epsilon_i-\Delta W_n(2\lambda)]}\right), \tag{22}$$

$$\langle n_2 2\lambda_2, i_2; k_1 m|B_{k_1 m}{}^{\dagger}|0\rangle = -\Lambda_{n_2}(2\lambda_2)\left(\frac{2\lambda_2+1}{2k_1+1}\right)^{1/2}\frac{1}{\epsilon_{k_1}+\epsilon_{i_2}-2\epsilon_{g_{9/2}}+\Delta W_{n_2}(2\lambda_2)}$$

$$\times\sum_{n,\lambda,k,i}\frac{(2\lambda+1)\Lambda_n{}^2(0\lambda)\begin{Bmatrix}i & k_2 & \lambda\\ k_1 & k & \lambda_2\end{Bmatrix}M(k_2i;\lambda)M(ki;\lambda_2)M(kk_1;\lambda)}{[\epsilon_{g_{9/2}}+\epsilon_{i_2}-\epsilon_i-\epsilon_{p_{1/2}}-\Delta W_n(0\lambda)][\epsilon_k+\epsilon_{i_2}-\epsilon_{p_{1/2}}-\epsilon_{g_{9/2}}+\Delta W_{n_2}(2\lambda_2)-\Delta W_n(0\lambda)]}, \tag{23}$$

$$\langle n_2 0\lambda_2; k_2; i_1 m|B_{i_1 m}{}^{\dagger}|0\rangle = -\Lambda_{n_2}(0\lambda_2)\left(\frac{2\lambda_2+1}{2k_1+1}\right)^{1/2}$$

$$\times\sum_{n,\lambda,k,k'}\frac{(2\lambda+1)\Lambda_n{}^2(0\lambda)\begin{Bmatrix}k & k_2 & \lambda\\ i_1 & k' & \lambda_2\end{Bmatrix}M(k_2k;\lambda)M(k'k;\lambda_2)M(k'i_1;\lambda)}{[\epsilon_{k'}+\epsilon_{g_{9/2}}-\epsilon_{i_1}-\epsilon_{p_{1/2}}-\Delta W_n(0\lambda)][\epsilon_k+\epsilon_{g_{9/2}}-\epsilon_{k_2}-\epsilon_{p_{1/2}}-\Delta W_n(0\lambda)][\epsilon_{k'}-\epsilon_{k_2}+\Delta W_{n_2}(0\lambda_2)-\Delta W_n(0\lambda)]}$$

$$+\sum_{n,\lambda,i,i'}\frac{(2\lambda+1)\Lambda_n{}^2(2\lambda)\begin{Bmatrix}i & k_2 & \lambda\\ i_1 & i' & \lambda_2\end{Bmatrix}M(k_2i;\lambda)M(i'i;\lambda_2)M(i'i_1;\lambda)}{[2\epsilon_{g_{9/2}}-\epsilon_{i_1}-\epsilon_{i'}-\Delta W_n(2\lambda)][2\epsilon_{g_{9/2}}-\epsilon_{k_2}-\epsilon_i-\Delta W_n(2\lambda)][\epsilon_{g_{9/2}}-\epsilon_{k_2}+\epsilon_{p_{1/2}}-\epsilon_{i'}+\Delta W_{n_2}(0\lambda_2)-\Delta W_n(2\lambda)]}, \tag{24}$$

$$\langle n_2 2\lambda_2; i_2; i_1 m|B_{i_1 m}{}^{\dagger}|0\rangle = \Lambda_{n_2}(2\lambda_2)\left(\frac{2\lambda_2+1}{2i_1+1}\right)^{1/2}\sum_{n,\lambda,k,i}$$

$$\times\frac{(2\lambda+1)\Lambda_n{}^2(0\lambda)\begin{Bmatrix}i & i_2 & \lambda\\ i_1 & k & \lambda_2\end{Bmatrix}M(k_2i;\lambda)M(ki;\lambda_2)M(ki_1;\lambda)}{[\epsilon_k+\epsilon_{g_{9/2}}-\epsilon_{i_1}-\epsilon_{p_{1/2}}-\Delta W_n(0\lambda)][\epsilon_{g_{9/2}}+\epsilon_{i_2}-\epsilon_i-\epsilon_{p_{1/2}}-\Delta W_n(0\lambda)][\epsilon_k-\epsilon_{g_{9/2}}-\epsilon_{p_{1/2}}+\epsilon_{i_2}+\Delta W_{n_2}(2\lambda_2)-\Delta W_n(0\lambda)]}. \tag{25}$$

In addition to the energy diagrams of Fig. 6 of Ref. 8, there exist disconnected self-energy diagrams for the particle and for the phonons. These diagrams are not included in the diagonalization of the effective Hamiltonian which is performed in Ref. 8, since empirical single-particle and phonon energies are used there. The diagrams corresponding to the inclusion of self-energy processes in the final particle (hole) are represented in Fig. 4. (Diagrams corresponding to the inclusion of self-energy terms in the particle that is transferred to the nucleus are given in Fig. 2.) Again the difference in spin and/or parity between single-particle and single-hole states reduces the number of total possible time permutations. There are only four for diagrams 4(a) and eight for diagrams 4(b). The matrix elements corresponding to Fig. 4(a)

are

$$\langle n_2 0\lambda_2; k_2; k_1 m|B_{k_1 m}{}^{\dagger}|0\rangle = -\Lambda_{n_2}(0\lambda_2)\frac{(2\lambda_2+1)^{1/2}}{(2k_1+1)^{1/2}(2k_2+1)}\frac{M(k_2k_1;\lambda_2)}{[\epsilon_{k_1}-\epsilon_{k_2}-\epsilon_{g_{9/2}}+\epsilon_{p_{1/2}}+\Delta W_{n_2}(0\lambda_2)]}$$
$$\times\left\{-\frac{1}{2}\sum_{n,\lambda,k}\frac{\Lambda_n{}^2(0\lambda)(2\lambda+1)M^2(kk_2;\lambda)}{[\epsilon_{g_{9/2}}-\epsilon_{p_{1/2}}+\epsilon_k-\epsilon_{k_2}-\Delta W_n(0\lambda)]^2}-\frac{1}{2}\sum_{n,\lambda,i}\frac{\Lambda_n{}^2(2\lambda)(2\lambda+1)M^2(ii_2;\lambda)}{[2\epsilon_{g_{9/2}}-\epsilon_i-\epsilon_{k_2}-\Delta W_n(2\lambda)]^2}\right\}, \tag{26}$$

$$\langle n_2 2\lambda_2; i_2; k_1 m|B_{k_1 m}{}^{\dagger}|0\rangle = \Lambda_{n_2}(2\lambda_2)\frac{(2\lambda_2+1)^{1/2}}{(2k_1+1)^{1/2}(2i_2+1)}\frac{M(i_2k_1;\lambda_2)}{[-2\epsilon_{g_{9/2}}+\epsilon_{k_1}+\epsilon_{i_2}+\Delta W_{n_2}(2\lambda_2)]}$$
$$\times\left\{-\frac{1}{2}\sum_{n,\lambda,i}\frac{\Lambda_n{}^2(0\lambda)(2\lambda+1)M^2(ii_2;\lambda)}{[\epsilon_{g_{9/2}}+\epsilon_{i_2}-\epsilon_{p_{1/2}}-\epsilon_i-\Delta W_n(0\lambda)]^2}-\frac{1}{2}\sum_{n,\lambda,k}\frac{\Lambda_n{}^2(-2\lambda)(2\lambda+1)M^2(ki_2;\lambda)}{[\epsilon_k-2\epsilon_{p_{1/2}}+\epsilon_{i_2}-\Delta W_n(-2\lambda)]^2}\right\}. \tag{27}$$

The matrix elements corresponding to Fig. 4(b) are

$$\langle n_2 0\lambda_2; k_2; i_1 m|B_{i_1 m}{}^{\dagger}|0\rangle = \Lambda_{n_2}(0\lambda_2)\frac{(2\lambda_2+1)^{1/2}}{(2i_1+1)^{1/2}(2k_2+1)}\frac{M(k_2i_1;\lambda_2)}{[\epsilon_{g_{9/2}}+\epsilon_{k_2}-\epsilon_{p_{1/2}}-\epsilon_{i_1}-\Delta W_{n_2}(0\lambda_2)]}$$
$$\times\left\{-\frac{1}{2}\sum_{n,\lambda,k}\frac{\Lambda_n{}^2(0\lambda)(2\lambda+1)M^2(kk_2;\lambda)}{[\epsilon_{g_{9/2}}-\epsilon_{p_{1/2}}+\epsilon_k-\epsilon_{k_2}-\Delta W_n(0\lambda)]^2}-\frac{1}{2}\sum_{n,\lambda,i}\frac{\Lambda_n{}^2(2\lambda)(2\lambda+1)M^2(ik_2;\lambda)}{[2\epsilon_{g_{9/2}}-\epsilon_{k_2}-\epsilon_i-\Delta W_n(2\lambda)]^2}\right\}, \tag{28}$$

$$\langle n_2 2\lambda_2; i_2; i_1 m|B_{i_1 m}{}^{\dagger}|0\rangle = -\Lambda_{n_2}(2\lambda_2)\frac{(2\lambda_2+1)^{1/2}}{(2i_1+1)^{1/2}(2i_2+1)}\frac{M(i_2i_1;\lambda_2)}{[2\epsilon_{g_{9/2}}-\epsilon_{i_1}-\epsilon_{i_2}-\Delta W_{n_2}(2\lambda_2)]}$$
$$\times\left\{-\frac{1}{2}\sum_{n,\lambda,i}\frac{\Lambda_n{}^2(0\lambda)(2\lambda+1)M^2(ii_1;\lambda)}{[\epsilon_{g_{9/2}}-\epsilon_{p_{1/2}}+\epsilon_{i_2}-\epsilon_i-\Delta W_n(0\lambda)]^2}-\frac{1}{2}\sum_{n,\lambda,k}\frac{\Lambda_n{}^2(-2\lambda)(2\lambda+1)M^2(ki_1;\lambda)}{[\epsilon_k+\epsilon_{i_2}-2\epsilon_{p_{1/2}}-\Delta W_n(-2\lambda)]^2}\right\}. \tag{29}$$

Note in Fig. 4 that, when the intermidiate particle k (hole i) is scattered by the other instead of being scattered by the same phonon, the resultant diagrams coincide with those of Fig. 3.

Finally, Fig. 5 includes those diagrams in which self-energy effects are included in the phonons. Probably these diagrams are the most interesting ones of the third-order perturbation, since they include those cases in which, for instance, two bosons of the same α and λ are present in the ground state [Fig. 5(c)]. It is important to note that the intermediate two-phonon states in graphs 5(c) do not represent the admixture of two-particle–two-hole states in the closes-shell nuclei, but rather the modification of the admixture predicted by the RPA. Since the RPA overestimates the ground-state correlations, it is through these processes of including admixtures of dressed phonon in the ground state that the formalism has the opportunity for correcting itself.

Each graph in Figs. 5(a) and 5(b) gives rise to 12 additional graphs by time-order permutation. The corresponding matrix elements are

$$\langle n_2 0\lambda_2; k_2; k_1 m|B_{k_1 m}{}^{\dagger}|0\rangle = -\Lambda_{n_2}(0\lambda_2)\left(\frac{2\lambda_2+1}{2k_1+1}\right)^{1/2}\frac{M(k_2k_1;\lambda_2)}{[\epsilon_{p_{1/2}}-\epsilon_{g_{9/2}}+\epsilon_{k_1}-\epsilon_{k_2}+\Delta W_{n_2}(0\lambda_2)]}$$
$$\times\sum_{n,\lambda,i}\frac{\Lambda_n{}^2(0\lambda_2)M^2(ki;\lambda_2)}{[\Delta W_{n_2}(0\lambda_2)-\Delta W_n(0\lambda_2)][\epsilon_k+\epsilon_{p_{1/2}}-\epsilon_{g_{9/2}}-\epsilon_i+\Delta W_{n_2}(0\lambda_2)]}, \tag{30}$$

$$\langle n_2 2\lambda_2; i_2; k_1 m|B_{k_1 m}{}^{\dagger}|0\rangle = \Lambda_{n_2}(2\lambda_2)\left(\frac{2\lambda_2+1}{2k_1+1}\right)^{1/2}\frac{M(i_2k_1;\lambda_2)}{[\epsilon_{k_1}+\epsilon_{i_2}-2\epsilon_{g_{9/2}}+\Delta W_{n_2}(2\lambda_2)]}$$
$$\times\sum_{n,k\geq k'}\frac{\Lambda_n{}^2(2\lambda_2)M^2(kk',\lambda_2)/[\delta(k,k')+1]}{[\Delta W_{n_2}(2\lambda_2)-\Delta W_n(2\lambda_2)][\epsilon_k+\epsilon_{k'}-2\epsilon_{g_{9/2}}+\Delta W_{n_2}(2\lambda_2)]}, \tag{31}$$

$$\langle n_2 0\lambda_2; k_2; i_1 m | B_{i_1 m}{}^{\dagger} | 0\rangle = \Lambda_{n_2}(0\lambda_2)\left(\frac{2\lambda_2+1}{2i_1+1}\right)^{1/2} \frac{M(k_2 i_1; \lambda_2)}{[\epsilon_{g_{9/2}} + \epsilon_{k_2} - \epsilon_{p_{1/2}} - \epsilon_{i_1} - \Delta W_{n_2}(0\lambda_2)]}$$
$$\times \sum_{n,k,i} \frac{\Lambda_n{}^2(0\lambda_2) M^2(ki; \lambda_2)}{[\Delta W_{n_2}(0\lambda_2) - \Delta W_n(0\lambda)][\epsilon_k + \epsilon_{p_{1/2}} - \epsilon_{g_{9/2}} - \epsilon_i + \Delta W_{n_2}(0\lambda_2)]}, \tag{32}$$

$$\langle n_2 2\lambda_2; i_2; i_1 m | B_{i_1 m}{}^{\dagger} | 0\rangle = -\Lambda_{n_2}(2\lambda_2)\left(\frac{2\lambda_2+1}{2i_1+1}\right)^{1/2} \frac{M(i_2 i_1; \lambda_2)}{[2\epsilon_{g_{9/2}} - \epsilon_{i_1} - \epsilon_{i_2} - \Delta W_{n_2}(2\lambda_2)]}$$
$$\times \sum_{n,k\geq k'} \frac{\Lambda_n{}^2(2\lambda_2) M^2(kk', \lambda_2)/[1+\delta(k,k')]}{[\Delta W_{n_2}(2\lambda_2) - \Delta W_n(0\lambda)][\epsilon_{k_1} + \epsilon_{k_2} - 2\epsilon_{g_{9/2}} + \Delta W_n(2\lambda_2)]}. \tag{33}$$

IV. RESULTS OF THE CALCULATION

We have used five particle-particle phonons ($\alpha = 2$) with $\lambda = 0$, 2, 4, 6, and 8, respectively, and a one-particle-hole phonon with $\lambda = 3$. The single-particle and phonon energies and the interaction constants $\Lambda_n(\alpha\lambda)$ [Eqs. (A11a) and (A11b)] are the same as in Ref. 8. It is worthwhile to remember that all these parameters have been experimentally determined from states having either one particle (hole) or one pairing boson. That is to say, there are no free parameters in the calculation.

We have used here the same mixture of perturbation theory and exact diagonalization which is discussed in Ref. 8. An effective Hamiltonian is constructed between states [Eqs. (1a) and (1b)]. This Hamiltonian is of second order in the interaction constants $\Lambda_n(\alpha\lambda)$. Therefore, some of the third-order graphs which appeared in the previous discussion must be eliminated in order not to take into account the same processes twice. Quite generally, we should omit those graphs in which we have a pure state [Eqs. (1a) or (1b)] (in ^{209}Pb) at a certain time and another state of our basis set of states in the same nucleus at a later time. Most of the graphs represented in Figs. 1–5 are thus eliminated (but not those obtained from them through different time ordering). Let us clarify this procedure with an example: If we consider the last graph 3(b), we have an intermediate state $|n0\lambda; k; i_1 m\rangle$ which eventually decays into the final $|n2\lambda_2; i_2; i_1 m\rangle$ state. Within our procedure, this same process will be carried out as follows: Once the effective Hamiltonian has been diagonalized, there will be a state having $|n2\lambda_2; i_2; i_1 m\rangle$ as the main component and $|n0\lambda; k; i_1 m\rangle$ as an admixture. Therefore, the third-order process [Fig. 3(b)] is equivalent to a first-order process [Fig. 1(b)] populating the (second-order) admixture $|n0\lambda; i_1 m\rangle$. From the 11 remaining graphs which appear as vertex permutations of the last graph of Fig. 3(b), only one other has to be suppressed, namely the one obtained from the figure by permuting the last two interactions.

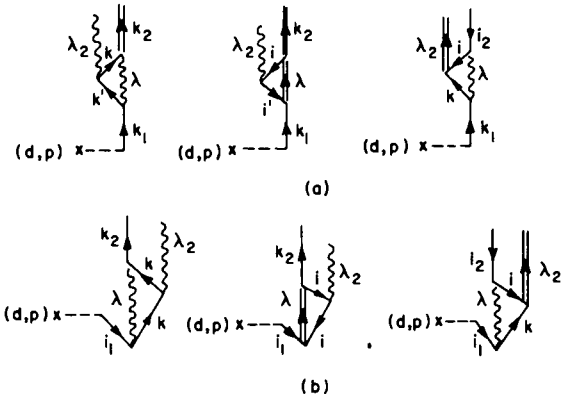

FIG. 3. Third-order graphs representing the one-body stripping reactions on closed-shell nuclei. The existence of these graphs, at difference with those displayed in Fig. 2, is required because of the overcompleteness of the 2p-1h basis used. The distinction between graphs of type (a) and (b) is the same as in Fig. 1.

Both the ^{207}Pb$(t,p)^{209}$Pb and the ^{210}Pb$(p,d)^{209}$Pb experimental results[12] clearly indicate that the $\frac{1}{2}^-$ state at 2.15 MeV is correctly represented by the $|120; p_{1/2}; \frac{1}{2}m\rangle$ wave function. Therefore, this is a very appropriate case to test our formalism. Table I contains the first-order matrix elements B_ν of the effective one-body-transfer operator. We see that transitions to different states belonging to our basis set are all of the same order of magnitude, irrespective of the "collectivity" that is carried by the state. According to the previous discussion, the first line of the last column in Table I corresponds to the (first-order) last graph 1(b), while the remaining lines of the same column represent third-order contributions 2(b) and 3(b).

In Table II, we compare the contributions to the stripping amplitude of different graphs. In the $\frac{1}{2}^-$ case, third-order contributions are down by a factor of 10 with respect to first-order contributions. For the $\frac{3}{2}^-$ and $\frac{5}{2}^-$ states, however, the convergence is not so good.

Table III includes our predictions to the lowest-states with the same spin and parity as the single-hole states in ^{208}Pb and excitation energy less than 4 MeV. The experimental spectroscopic factors

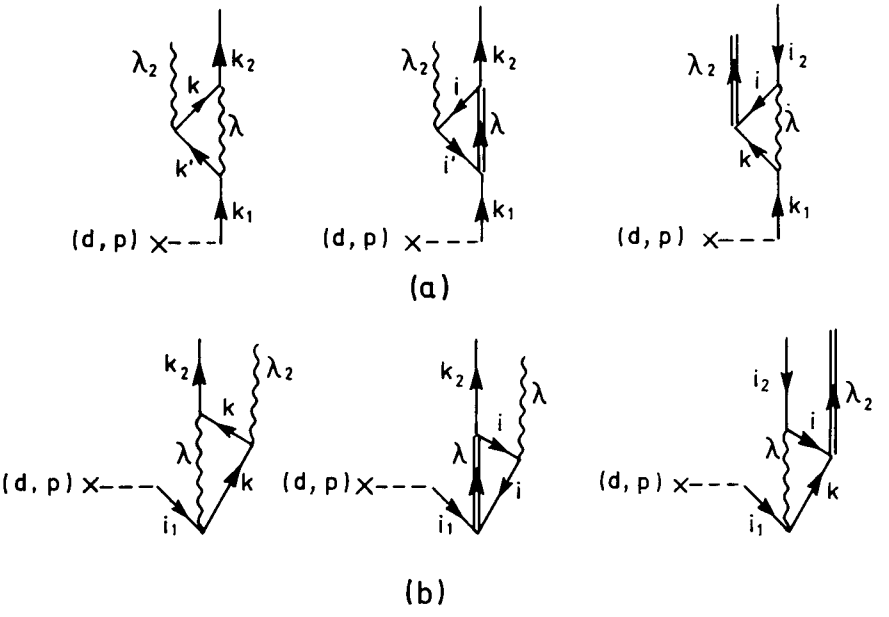

FIG. 4. Third-order graphs representing the one-body stripping reactions on closed-shell nuclei. These graphs take into account self-energy processes in the particle (hole) of the 2p-1h final state. The distinction between graphs of type (a) and (b) is the same as in Fig. 1.

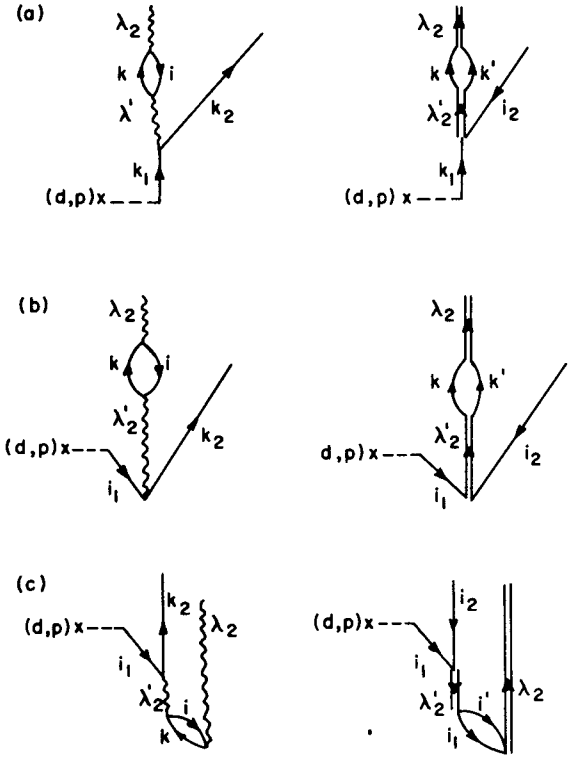

FIG. 5. Third-order graphs representing the one-body stripping reactions on closed-shell nuclei. Graphs (a) and (b) take into account self-energy processes in the phonon of the 2p-1h final state. Graphs (c) correspond to the admixture of two-phonon states in the vacuum state. The distinction between graphs of type (a) and (b) is the same as in Fig. 1.

TABLE I. The contribution of the first-order graphs 1(b) to the effective one-body stripping transfer matrix elements to components $\nu = (n\alpha\lambda; j; \frac{1}{2}m)$ of the $\frac{1}{2}^-$ state at 2.15[2] MeV in ^{209}Pb. The second column gives the amplitudes of the unperturbed state ν in the lowest $\frac{1}{2}^-$ state. The third column contains the values of the matrix elements discussed in Sec. III and displayed in Fig. 1(b) (first order).

n	α	λ	l_j	α_ν	$B^{\frac{1}{2}}_\nu$	$a_\nu B^{\frac{1}{2}}_\nu$
1	2	0	$p_{1/2}$	−0.999	−0.100	0.100
1	2	2	$p_{3/2}$	0.022	−0.069	−0.0015
1	2	2	$f_{5/2}$	0.034	−0.081	−0.0029
1	2	4	$h_{9/2}$	0.005	−0.033	−0.0002
1	2	4	$f_{7/2}$	0.010	−0.046	−0.0005
1	0	3	$d_{5/2}$	0.024	0.137	0.0028
1	0	3	$g_{7/2}$	0.005	0.142	0.0006
						0.099

TABLE II. The contribution of graphs 1(b)–5(b) to the total one-body stripping spectroscopic amplitude for the transition populating the lowest states with $J^\pi = \frac{1}{2}^-$, $\frac{3}{2}^-$, and $\frac{5}{2}^-$ in ^{209}Pb. We list the sum $\sum_\nu a_\nu^{(n)} B_\nu^{(n)}$ ($n = 1$ and 3) where a_ν is the amplitude of the unperturbed states $\nu = (n\alpha\lambda; j; Jm)$.

Graphs	$\sum_{n,\nu} a_\nu^{(n)} B_\nu^{(n)}$ $\frac{1}{2}^-$	$\frac{3}{2}^-$	$\frac{5}{2}^-$
1(b)	0.099	0.168	0.069
2(b)	−0.015	−0.061	−0.007
3(b)	0.009	0.024	0.009
4(b)	−0.011	−0.009	−0.004
5(b)	0.010	0.090	0.033
	0.092	0.252	0.100

were obtained with the usual separation-energy method, which may be completely wrong in this case. For instance, in the case of the $J^\pi = \frac{1}{2}^-$ state of ^{209}Pb at 2.152 MeV, the single-particle level is given a separation energy of ≈1.7 MeV instead of 7.3 MeV corresponding to the position in a realistic well.

The predicted population of the states having an $\alpha = 2$ phonon in the main component is in reasonable agreement with the experimental numbers. However, the predictions for the transitions to $\alpha = 0$, $\lambda = 3$ states is overestimated by a factor of 10.

Only $\frac{15}{2}^-$ states are predicted among the states of ^{209}Pb having the same spin and parity as the single-particle states with an energy below 4 MeV. From the discussion in Ref. 8, it became clear that the predicted mixture between the $|128; p_{1/2}; \frac{15}{2}m\rangle$ state and the $|103; g_{9/2}; \frac{15}{2}m\rangle$ and $|103; i_{11/2}; \frac{15}{2}m\rangle$ states is not sufficient to account for the empirical (t, p) or

TABLE III. Energies and single-stripping spectroscopic factors of those 2p–1h states of ^{209}Pb [reached in the ^{208}Pb-(d,p) reaction] having the spin and parity of single-hole states. For each J^π, the first and second lines give the excitation energy (MeV) and the spectroscopic factor, respectively. The remaining lines contain the amplitudes $a(1\alpha\lambda; j; J)$ of some unperturbed states. States up to 4 MeV have been included.

$J^\pi = \frac{1}{2}^-$	Theory			Experiment		
E	2.22	3.57	3.83		2.15	
S	0.009	0.008	0.016	0.007 [a]	0.06 [b]	0.005 [c]
$a(120; p_{1/2}; \frac{1}{2})$	1.00	0.03	0.01			

$J^\pi = \frac{3}{2}^-$	Theory					Experiment [a]	
E	2.40	2.98	3.21	3.55	3.79	2.32	3.08
S	0.063	0.000	0.000	0.000	0.002	0.007	0.002
$a(122; p_{1/2}; \frac{3}{2})$	−0.115	0.971	−0.201	0.033	0.016		
$a(120; p_{3/2}; \frac{3}{2})$	0.339	0.237	0.900	−0.091	−0.040		
$a(103; g_{9/2}; \frac{3}{2})$	0.910	0.028	−0.311	0.101	0.038		

$J^\pi = \frac{5}{2}^-$	Theory					Experiment [a]		
E	2.90	2.79	2.98	3.41	3.60	2.46	2.74	2.88
S	0.010	0.006	0.004	0.024	0.001	0.001	0.003	0.001
$a(122; p_{1/2}; \frac{5}{2})$	0.045	−0.142	0.987	0.023	−0.039			
$a(120; f_{5/2}; \frac{5}{2})$	0.221	0.957	0.120	0.107	−0.088			
$a(103; g_{9/2}; \frac{5}{2})$	0.961	−0.208	−0.071	0.011	0.028			

$J^\pi = \frac{7}{2}^-$	Theory				
E	2.64	3.22	3.25	3.56	3.79
S	0.013	0.0003	0.002	0.0000	0.0001
$a(124; p_{1/2}; \frac{7}{2})$	−0.077	+0.995	0.049	−0.007	0.005
$a(103; g_{9/2}; \frac{7}{2})$	0.943	−0.064	0.102	0.017	0.009

$J^\pi = \frac{9}{2}^-$	Theory				
E	2.49	3.21	3.42	3.56	3.79
S	0.001	0.001	0.009	0.0000	0.0001
$a(124; p_{1/2}; \frac{9}{2})$	0.039	0.993	0.104	0.033	0.005
$a(103; g_{9/2}; \frac{9}{2})$	0.993	0.035	−0.018	−0.051	−0.027

$J^\pi = \frac{13}{2}^+$	Theory
E	3.83
S	0.005
$a(120; i_{13/2}; \frac{13}{2})$	

[a] N. Stein and D. Kovar, private communication. The measured cross sections have an error of 10%. However, the spectroscopic factor may carry a much larger uncertainty associated with its derivation through the DWBA.

[b] G. J. Igo, P. D. Barnes, E. R. Flynn, and D. D. Armstrong, Phys. Rev. 177, 1831 (1969).

[c] C. Ellegaard and P. Vedelsby, Phys. Letters 26B, 155 (1968).

TABLE IV. Transitions to 2p-1h of ^{209}Pb states having $J^\pi = \frac{15}{2}^-$ and excited in the reaction ^{208}Pb(d,p).

$J^\pi = \frac{15}{2}^-$	Theory				Experiment [a]		
E	3.22	3.32	3.47	3.85	3.06	3.56	3.72
S	0.17	0.001	0.30	0.002	0.10	0.05	0.05
$a(128; p_{1/2}; \frac{15}{2})$	0.065	0.987	0.141	−0.010			
$a(103; g_{9/2}; \frac{15}{2})$	0.698	0.057	−0.712	0.027			
$a(103; i_{11/2}; \frac{15}{2})$	0.711	−0.145	0.687	0.006			

[a] N. Stein and D. Kovar, private communication. (See comments in Ref. a, Table III.)

(p, d) cross sections to the 3.56- and 3.72-MeV states in ^{209}Pb (the corresponding theoretical energies are 3.32 and 3.47 MeV, respectively). The (d, p) data (Table IV) confirms this difficulty of the model.

The pickup reaction ^{208}Pb$(p, d)^{207}$Pb leading to 1p-2h states in ^{207}Pb may obviously be treated within the same coupling scheme. The corresponding results are summarized in Tables V and VI. Some of the predicted cross sections have been identified experimentally and our results are in reasonable agreement with the empirical numbers. It is apparent from Tables V and VI that a larger number of states is expected to be populated by the pickup reaction below 5 MeV. Although many states have been seen,[13] to our knowledge, spin, parities, and spectroscopic factors are not yet available.

V. CONCLUSIONS

In this paper we have attempted to explain the one-body transfer transitions that are forbidden within the framework of a pure independent-particle model, by the coupling between particles and phonons. Our calculation yields spectroscopic factors. The comparison of these with the experimental numbers is handicapped by the approximations involved in the usual DWBA (such as separation-energy procedure and the neglect of inelastic processes). Until a more careful treatment of these effects is done, we can only expect an agreement in the order of magnitude. This is indeed the case for the results shown in Tables III–VI.

ACKNOWLEDGMENTS

We are grateful to N. Stein and D. Kovar for providing us with unpublished experimental results.

APPENDIX A

The multipole particle-hole and pairing Hamiltonians are

$$H(2\lambda) = -G_\lambda \pi (2\lambda+1) \sum_\mu P_{\lambda\mu}{}^\dagger P_{\lambda\mu}, \tag{A1}$$

$$H(0\lambda) = \frac{X_\lambda}{2} \sum_\mu Q_{\lambda\mu} Q_{\lambda\mu}{}^\dagger, \tag{A2}$$

where $Q_{\lambda\mu}$ and $P_{\lambda\mu}{}^\dagger$ are defined in Eqs. (8) and (9). The collective and noncollective operators are

$$\beta_n{}^\dagger(2\lambda\mu) = \sum_{k_1 \geq k_2} d_n(k_1 k_2; 2\lambda) \beta^\dagger(k_1 k_2; 2\lambda\mu) - (-1)^{\lambda-\mu} \sum_{i_1 \geq i_2} d_n(i_1 i_2; 2\lambda) \beta(i_1 i_2; 2\lambda -\mu), \tag{A3a}$$

$$\beta_n{}^\dagger(-2\lambda\mu) = \sum_{i_1 \geq i_2} d_n(i_1 i_2; -2\lambda) \beta^\dagger(i_1 i_2; -2\lambda\mu) - (-1)^{\lambda-\mu} \sum_{k_1 \geq k_2} d_n(k_1 k_2; -2\lambda) \beta(k_1 k_2; -2\lambda -\mu), \tag{A3b}$$

$$\beta(0\lambda\mu) = \sum_{k,i} d_n(k_1 i; 0\lambda) \beta^\dagger(ki; 0\lambda\mu) - (-1)^{\lambda-\mu} \sum_{k,i} d_n(ik; 0\lambda) \beta(ki; 0\lambda -\mu), \tag{A4}$$

$$\beta^\dagger(k_1 k_2; 2\lambda\mu) = \frac{1}{(1+\delta_{12})^{1/2}} (b_{k_1}{}^\dagger b_{k_2}{}^\dagger)^\lambda_\mu, \tag{A5a}$$

$$\beta^\dagger(i_1 i_2; -2\lambda\mu) = \frac{1}{(1+\delta_{12})^{1/2}} (b_{i_1} b_{i_2})^\lambda_\mu, \tag{A5b}$$

$$\beta^\dagger(ki; 0\lambda\mu) = (b_k{}^\dagger b_i)^\lambda_\mu. \tag{A6}$$

The coefficients $d_n(j_1 j_2; \alpha\lambda)$ are determined by the linearization equations

$$[H(\alpha\lambda), \beta^\dagger(\alpha\lambda)] = W_n(\alpha\lambda) \beta^\dagger(\alpha\lambda), \tag{A7}$$

and are equal to

$$d_n(k_1 k_2; 2\lambda) = \frac{\Lambda_n(2\lambda)}{(1+\delta_{12})^{1/2}} \frac{M(k_1 k_2; \lambda)}{E_{k_1 k_2} - W_n(2\lambda)}, \tag{A8a}$$

$$d_n(i_1 i_2; 2\lambda) = \frac{\Lambda_n(2\lambda)}{(1+\delta_{12})^{1/2}} \frac{M(i_1 i_2; \lambda)}{E_{i_1 i_2} + W_n(2\lambda)}, \tag{A8b}$$

TABLE V. Transitions corresponding to the reaction ^{208}Pb(p,d) to 1p-2h states of ^{207}Pb having the spin and parity of the single-particle states and predicted excitation energy below 5 MeV.

$J^\pi = \frac{9}{2}^+$	Theory						Experiment [a]
E	2.76	3.23	3.54	3.77	4.35	4.76	2.74
S	0.11	0.01	0.13	0.09	0.0005	0.005	0.052
$a(1\text{-}20; g_{9/2}; \frac{9}{2})$	0.975	0.126	−0.074	−0.159	−0.004	0.010	
$a(103; f_{5/2}; \frac{9}{2})$	−0.147	0.974	0.029	−0.135	0.077	0.015	
$a(1\text{-}20; i_{11/2}; \frac{9}{2})$	−0.002	−0.094	0.872	−0.479	−0.007	0.016	
$a(103; p_{3/2}; \frac{9}{2})$	0.163	0.128	0.477	0.829	0.063	−0.024	
$J^\pi = \frac{11}{2}^+$							
E	3.27	3.57	3.61	4.37	4.45		
S	0.27	0.0000	0.0000	0.015	0.0001		
$a(103; f_{5/2}; \frac{11}{2})$	0.921	0.04	−0.370	−0.090	0.033		
$a(1\text{-}22; g_{9/2}; \frac{11}{2})$	0.054	0.967	0.247	0.006	0.000		
$a(1\text{-}20; i_{11/2}; \frac{11}{2})$	0.376	−0.249	0.892	0.036	−0.010		
$J^\pi = \frac{15}{2}^-$							
E		4.17			4.31		
S		0.09			0.12		
$a(1\text{-}20; j_{15/2}; \frac{15}{2})$		0.939			−0.344		
$a(103; i_{13/2}; \frac{15}{2})$		0.314			0.938		
$J^\pi = \frac{5}{2}^+$							
E	2.67	3.26	3.56	3.75	4.37	8.47	
S	0.07	0.04	0.03	0.02	0.007	0.004	
$a(103; p_{1/2}; \frac{5}{2})$	0.961	0.042	0.128	0.199	+0.098	0.043	
$a(103; f_{5/2}; \frac{5}{2})$	−0.102	0.965	0.167	0.118	+0.037	0.093	
$a(1\text{-}20; d_{5/2}; \frac{5}{2})$	−0.223	−0.231	0.722	0.606	+0.061	0.044	
$a(103; p_{3/2}; \frac{5}{2})$	0.088	−0.002	0.652	−0.728	−0.081	−0.039	

$J^\pi = \frac{1}{2}^+$	Theory				Experiment [a]
E	3.43	4.49	4.76	4.88	3.29
S	0.02	0.0000	0.04	0.02	0.10
$a(103; f_{5/2}; \frac{1}{2})$	0.945	0.194	0.095	−0.187	
$a(1\text{-}24; g_{9/2}; \frac{1}{2})$	−0.182	0.963	−0.184	0.036	
$J^\pi = \frac{7}{2}^+$					
E	2.73	3.28	3.59	3.62	4.38	4.46
S	0.06	0.06	0.04	0.03	0.003	0.0003
$a(103; p_{1/2}; \frac{7}{2})$	0.977	+0.132	−0.134	0.053	−0.106	0.033
$a(103; f_{5/2}; \frac{7}{2})$	−0.194	0.889	−0.390	0.071	−0.059	0.064
$a(1\text{-}22; g_{9/2}; \frac{7}{2})$	0.037	0.305	0.776	0.550	0.012	−0.010
$J^\pi = \frac{3}{2}^+$						
E	3.27	3.97	4.45	4.68		
S	0.008	0.05	0.003	0.03		
$a(103; f_{5/2}; \frac{3}{2})$	0.934	0.295	−0.165	0.023		
$a(103; p_{3/2}; \frac{3}{2})$	−0.327	0.890	−0.151	0.228		
$a(1\text{-}24; g_{9/2}; \frac{3}{2})$	0.122	0.116	0.923	0.343		

[a] S. M. Smith, P. G. Roos, C. Moazed, and A. M. Bernstein, to be published. The error in the absolute cross sections is ≈10%. Concerning the possible error of the spectrscopic factors see Table III.

TABLE VI. Energies and spectroscopic factors corresponding to the ^{208}Pb(p,d) reaction exciting 1p-2h of ^{207}Pb states having the spin and parity of the single-hole states and predicted excitation energy below 5 MeV.

$J^\pi = \frac{7}{2}^-$	Theory	Experiments [a]
E	4.67	4.52
S	2.61	0.8
$a(103;\ i_{13/2};\ \frac{7}{2})$	0.997	
$J^\pi = \frac{9}{2}^-$		
E		4.22
S		0.99
$a(103;\ i_{13/2};\ \frac{9}{2})$		1.00

$J^\pi = \frac{13}{2}^+$	Theory		
E	3.62	4.34	4.46
S	0.35	0.01	0.06
$a(1\text{-}22;\ g_{9/2};\ \frac{13}{2})$	0.99	−0.010	0.020
$a(1\text{-}22;\ i_{11/2};\ \frac{13}{2})$	0.011	0.999	−0.032
$a(1\text{-}20;\ g_{9/2};\ \frac{13}{2})$	0.021	0.032	0.999

[a] S. M. Smith, P. G. Roos, C. Moazed, and A. M. Bernstein, to be published. The error in the absolute cross sections is ≈10%. Concerning the possible error of the spectroscopic factors see Table III.

$$d_n(i_1 i_2; -2\lambda) = \frac{\Lambda_n(-2\lambda)}{(1+\delta_{12})^{1/2}} \frac{M(i_1 i_2; \lambda)}{E_{i_1 i_2} - W_n(-2\lambda)}, \tag{A9a}$$

$$d_n(k_1 k_2; -2\lambda) = \frac{\Lambda_n(-2\lambda)}{(1+\delta_{12})^{1/2}} \frac{M(k_1 k_2; \lambda)}{E_{k_1 k_2} + W_n(-2\lambda)}, \tag{A9b}$$

$$d_n(ki; 0\lambda) = \Lambda_n(0\lambda) \frac{M(ki; \lambda)}{E_{ki} - W_n(0\lambda)}, \tag{A10a}$$

$$d_n(ik; 0\lambda) = \Lambda_n(0\lambda) \frac{M(ki; \lambda)}{E_{ki} + W_n(0\lambda)}. \tag{A10b}$$

From the normalization condition

$$\sum_{j_1 j_2} d_n^2(j_1 j_2; \alpha\lambda) - \sum_{j_3 j_4} d_n^2(j_3 j_4; \alpha\lambda) = 1,$$

we obtain the coupling strengths Λ that appear in $h(\alpha\lambda)$ [see Eqs. (6)–(9)]. They are equal to

$$\Lambda_n(\pm 2\lambda) = \sqrt{2} \left\{ \pm \sum_{k_1 \geq k_2} \frac{|M(k_1, k_2; \lambda)|^2}{[E_{k_1 k_2} \mp W_n(\mp 2\lambda)]^2} \mp \sum_{i_1 \geq i_2} \frac{|M(i_1 i_2; \lambda)|^2}{[E_{i_1 i_2} \pm W_n(\pm 2\lambda)]^2} \right\}^{-1/2}, \tag{A11a}$$

$$\Lambda_n(0\lambda) = \left(\sum_{k \geq i} |M(ki; \lambda)|^2 \left\{ \frac{1}{[E_{ki} - W_n(0\lambda)]^2} + \frac{1}{[E_{ki} + W_n(0\lambda)]^2} \right\} \right)^{-1/2}. \tag{A11b}$$

*Work performed under the auspices of the U. S. Atomic Energy Commission.

†Present address: Niels Bohr Institute, University of Copenhagen, Copenhagen, Denmark.

[1] See for example, C. E. Ellegaard, J. Kantele, and P. Vedelsby, Phys. Letters 25B, 512 (1967); J. C. Hafele and R. Woods, *ibid.* 20, 674 (1966).

[2] See for example, O. Hansen, Ph.D. dissertation, Munskgaard, Copenhagen, 1967 (unpublished).

[3] R. J. Ascuitto and N. K. Glendenning, Phys. Rev. 181, 1396 (1969); T. Tamura, Ann. Rev. Nucl. Sci. 19, 99 (1969).

[4] I. Hamamoto, Nucl. Phys. A126, 545 (1969); A135, 576 (1969); A141, 1 (1970).

[5] B. R. Mottelson, J. Phys. Soc. Japan, Suppl. 24, 87 (1968).

[6] D. R. Bes and R. A. Broglia, to be published.

[7] R. Ibarra and B. Bayman, Phys. Rev. C 1, 1786 (1970).

[8] D. R. Bes and R. A. Broglia, Phys. Rev. C 3, 2349 (1971).

[9] G. E. Brown, J. A. Evans, and D. J. Thouless, Nucl. Phys. 45, 164 (1963); D. Zawischa and E. Werner, *ibid.* A125, 383 (1969); A. Goswami, A. Nacioglu, and A. Sherwood, to be published.

[10] B. R. Mottelson, *Topics in Nuclear Structure Theory, Nikko Summer School Lectures, 1967,* Nordita Publications No. 288.

[11] If $\alpha = \alpha_2$, $n = n_2$, $\lambda = \lambda_2$, and $j = j_2$, a denominator vanishes in Eqs. (18), (19), (20), and (11). In this case, we must replace the vanishing denominator by $-\frac{1}{2}$ of the denominator which is squared in the same equation. A similar change must be made in Eqs. (22), (24), (30), and (33) for those quantum numbers corresponding to a vanishing denominator.

[12] E. R. Flynn, G. Igo, P. D. Barnes, D. Kovar, D. Bes, and R. Broglia, preceding paper, Phys. Rev. C 3, 2371 (1971).

[13] W. P. Alford and D. G. Burke, Phys. Rev. 185, 1560 (1969).